## PAPER

# Fabrication of biocompatible magneto-fluorescence nanoparticles as a platform for fluorescent sensor and magnetic hyperthermia applications

Arphaphon Sichamnan,[a] Nararat Yong,[b] Siwapech Sillapaprayoon,[c] Wittaya Pimtong,[c] I.-Ming Tang,[d] Weerakanya Maneeprakorn ✶[b] and Weeraphat Pon-On ✶[a]

Multifunctional nanoparticles with special magnetic and optical properties have been attracting a great deal of attention due to their important applications in the bioanalytical and biomedical fields. In this study, we report the fabrication of biocompatible magneto-fluorescence nanoparticles consisting of carbon dots (CDots) and silica-coated cobalt–manganese nanoferrites ($Co_{0.5}Mn_{0.5}Fe_2O_4$) (CoMnF@Si@CDots) (MagSiCDots) by a facile hydrothermal method. The as-prepared MagSiCDots have a particle size of 100–120 nm and show a negative zeta potential of −35.50 mV at a neutral pH. The fluorescence spectrum of the MagSiCDots nanoparticles consists of sharp excitation at 365 nm and broad blue light emission with a maximum wavelength of 442.5 nm and the MagSiCDots exhibit superparamagnetic behaviour with a saturation magnetization of 11.6 emu $g^{-1}$. The potential of MagSiCDots as a fluorescent sensor and be used for magnetic hyperthermia applications. It is seen that the fluorescent intensity of a colloidal solution (a hydrogen sulfide ($H_2S$) solution containing MagSiCDots nanoparticles) has a linear relationship with the $H_2S$ concentration range of 0.2–2 μM. The limit of detection (LOD) of $H_2S$ by our MagSiCDots particles is 0.26 μM and they remain stable for at least 90 min. To test the suitability of the MagSiCDots nanoparticles for use in hyperthermia application, induction heating using an AMF was done. It was observed that these nanoparticles had a specific absorption rate (SAR) of 28.25 W $g^{-1}$. The *in vitro* and *in vivo* cytotoxicity of MagSiCDots were tested on HeLa cells lines. The results show a cell viability of about 85% when exposed to 100 μg $mL^{-1}$ concentration of the particles. The *in vivo* cytotoxicity using zebrafish assay also confirmed the non-toxicity and biocompatibility of the nanoparticles to living cells. The reported data demonstrate that by combining CoMnF@Si and fluorescent CDots into a single system, not only nontoxic multifunctional nanomaterials but also multimodal nanoparticles for several applications, such as hazard gas detection and acting as a biocompatible heat source for therapeutic treatment of cancer, are provided.

## 1. Introduction

The research on the development of nanomaterials with multifunctionalities has attracted much attention due to its great potential application for early detection and therapeutic functions in various biological fields.[1–3] Based on this strategy,

*[a]Department of Physics, Faculty of Science, Kasetsart University, Bangkok 10900, Thailand. E-mail: fsciwpp@ku.ac.th*

*[b]National Nanotechnology Center (NANOTEC), National Science and Technology Development Agency (NSTDA), Pathum Thani 12120, Thailand. E-mail: weerakanya@nanotec.or.th*

*[c]Nano Environmental and Health Safety Research Team, National Nanotechnology Center (NANOTEC), National Science and Technology Development Agency (NSTDA), Pathum Thani 12120, Thailand*

*[d]Department of Physics, Faculty of Science, Mahidol University, Bangkok 10400, Thailand*

magneto-fluorescent platform particles consisting of a magnetic core and fluorescent quantum dot shell have drawn much interest in last decade.[1–7] Magnetic inverse ferrite particles ($[M_{1-\delta}^{2+}Fe_\delta^{3+}][M_\delta^{2+}Fe_{2-\delta}^{3+}]O_4$ where $\delta$ is the degree of inversion) have attracted increasing attention due to their having wide applications such as in drug delivery, magnetic hyperthermia, environment sensors, MRI, the removal of heavy ions from water, the removal of microalgae, the sorting as well as detection of cells *etc.*[8–10] In addition, these magnetic nanoparticles have been used as biosensors since they be easily removed (separated at specific locations). For fluorescent particles, semiconductor nanocrystals composed of II–VI or III–V group elements (*e.g.* CdSe, CdS, CdTe, PbS, Cd–Te-(S,Se) *etc.*) have been used as fluorophore emitting sources.[11–14] However, individual ions such as $Cd^{2+}$, $Se^{2-}$, $Pb^{2+}$ and $Te^{2+}$ are reported to be cytotoxic (generally nontoxic concentrations are below sub

µg mL$^{-1}$ or even ng mL$^{-1}$).[1] Moreover, the large size of particles could interfere with the intracellular function. For this reason, nontoxic fluorescent agents have been researched. Carbon quantum dots (CQDs) (a new class of smaller dimensional carbon materials) have been attracting increasing attention because of their great potential in many research fields such as sensing or photoelectronics due to their superior fluorescent properties. In addition, CQDs exhibit high biocompatibility, water dispersibility and low-cost production.[15–17] Recently, magneto-fluorescent particles (the combination of CQDs and magnetic nanohybrids) have been proposed as a multifunctional magneto-fluorescence particle for biological and biomedical application. There are many reports on the synthesis of magneto-fluorescence hybrid/composite nanoparticles. For example, Hui Wang et al.,[18] have successfully synthesized magnetic Fe$_3$O$_4$ nanocrystals and fluorescent carbon dots (CDs) hybrid for fluorescent imaging and photothermal treatment. Ilana Perelshtein et al.,[19] have developed a new hybrid composite based on C-dots with magnetic Fe. They obtained highly magnetic particles which exhibited strong fluorescent properties. These particles could serve as a potential candidate for bioimaging applications and in diagnostic devices. Avijit Pramanik et al.,[20] reported the synthesis of red/blue fluorescent carbon dot (CD)-attached magnetic nanoparticle-based multicolor multifunctional CD-based nanosystems. Their data show that multicolor multifunctional CD-based nanosystems were capable of isolating MRSA and Salmonella DT104 superbugs from whole blood samples, followed by accurate identification via multicolor fluorescence imaging. Hanchun Yao et al.,[21] constructed magnetic-carbon quantum dots for bioimaging and targeted therapy. Mukesh Lavkush Bhaisare et al.,[22] tried to synthesized Mag-CDs for use in detecting pathogenic bacteria and demonstrated that the Mag-CDs were highly sensitive probes for bacterial detection. However, their difficulties of surface modifications of magneto-fluorescence nanoparticles could limit their uses especially in biomedical applications and sensing that require immobilization of biological moieties on the particle surfaces. Thus, other functionalized or coating substrates have allowed one to overcome several those limitations. Among them, silica-based nanomaterials provide an excellent choice because of their chemical stability, large surface area, biocompatibility, and ease of surface modification. Silica-coated magneto-fluorescence nanoparticles not only provide the biocompatibility of the particles but also preserve the fluorescence and magnetic properties resulting the improvement of particle stability. For instance, Sasmita Mohapatra et al.,[23] successful synthesized carbon quantum dots of Fe$_3$O$_4$@SiO$_2$@carbon quantum dots for use fluorescent fluoride ion sensing and were biocompatible. Meanwhile, Xiaolei Li, et al.,[24] synthesized Fe$_3$O$_4$@SiO$_2$@mSiO$_2$-organosilanes carbon dots and the potential to be used as a sensor and in drug delivery system. Yuxia Guan and colleagues[25] synthesized multifunctional magnetic fluorescent nanocomposite particles of Fe$_3$O$_4$@SiO$_2$-CDs as effective carrier of gambogic acid for inhibiting VX2 tumor cells. Experimental results shown that the bifunctional magnetic nanoparticles have an excellent fluorescence, magnetic properties and an outstanding magnetic targeting effect on tumors. Ashish Tiwari et al.,[26] demonstrated that the engineering of the magneto-fluorescent properties simply by tuning the carbon structure in graphitic carbon coated superparamagnetic iron oxides (SPIONs) and useful as a theranostic platform having the capability to enhance the specificity and efficacy of hyperthermia.

In this study, the magnetic-fluorescent particle of carbon dots (CDots) combined with silica-coated cobalt–manganese nanoferrite (Co$_{0.5}$Mn$_{0.5}$Fe$_2$O$_4$) (CoMnF@Si@CDots) (MagSiCDots) were synthesized for use as a sensitive fluorescent sensor for hydrogen sulfide (H$_2$S) and as a potential heat source for magnetic hyperthermia applications. H$_2$S is colourless, water soluble and is a flammable gas. Endogenous H$_2$S is a molecule generated by many tissues in human.[27–29] The abnormal level of H$_2$S is one of the symptoms of many diseases, such as diabetes, Down syndrome, Alzheimer disease and cancer.[30–32] The analysis of H$_2$S in physiological medical pathological events is essential to the diagnosis and to the understanding of related diseases fluorophores, carbon nanodots have recently been introduced. The usual analytical methods such as gas chromatography, electrochemistry or colorimetric have been used for H$_2$S detection. However, complex and long-time sample procedure are sparse. New approaches based on fluorescence techniques, organic of H$_2$S in real-time and offers high sensitivity monitoring in living systems.[33–35] The cobalt–manganese nanoferrite (Co$_{0.5}$Mn$_{0.5}$Fe$_2$O$_4$) in the hybrid nanoparticles serves two purposes. It can be used to affect magnetic separation and act as the heat source in a high efficacy magnetic hyperthermia (MH) therapy treatment. Also, cobalt-based nanoferrites show stability against oxidation, have low cytotoxicity and be strongly responsive to external magnetic fields.[36,37] Herein, the magneto-fluorescent MagSiCDots was synthesized via the hydrothermal method involving the MagSi and citric acid (carbon precursor). The resulting powder have a core–shell structure and emit a blue-green light emission. The fluorescent tension of MagSiCDots/H$_2$S system depends linearly with the H$_2$S in the range 0.2 to 2 µM and remain stable for at least 90 min. The possibility of hyperthermia application arises since an induction heating analysis of the MagSiCDots nanoparticles shows that the specific heat absorption rate (SAR) is 28.25 W g$^{-1}$. A potential candidate for various biomedical applications, the cytotoxicity of MagSiCDots in vitro and in vivo were tested on HeLa cells lines and using zebrafish assay were studied and exhibited nontoxic nature to the samples.

## 2. Materials and methods

### 2.1 Materials

The reagents for the hybrids were iron(III) chloride hexahydrate (FeCl$_3$·6H$_2$O) (Sigma-Aldrich, Germany), cobalt(III) chloride hexahydrate (CoCl$_2$·6H$_2$O) (Sigma-Aldrich, Germany), manganese(II) nitrate tetrahydrate (Mn(NO$_3$)$_2$·4H$_2$O) (PRS Panreac, Spain), ammonium hydroxide (NH$_4$OH) (ORëC, New Zealand), citric acid (C$_6$H$_8$O$_7$) (Merck, Germany), urea (CH$_4$N$_2$O) (KEMAUS, Australia), tetraethyl orthosilicate (Si(OC$_2$H$_5$)$_4$) (TEOS) (Sigma-Aldrich, Germany), ethanol. The above

chemicals were used to fabricate the carbon dots (CDots)/silica-coated cobalt–manganese nanoferrite ($Co_{0.5}Mn_{0.5}Fe_2O_4$) (CoMnF@Si@CDs) (MagSiCDots) particles via was prepared via a facile hydrothermal method. The final product had a core–shell structure. The fabrication process is shown in Fig. 1.

## 2.2 Preparation of cobalt–manganese nanoferrite ($Co_{0.5}Mn_{0.5}Fe_2O_4$) (Mag) nanoparticles

Magnetic $Co_{0.5}Mn_{0.5}Fe_2O_4$ nanoparticles (Mag) were synthesized via a standard hydrothermal method. Synthesis step, $FeCl_3 \cdot 6H_2O$ (1.35 g), $CoCl_2 \cdot 6H_2O$ (0.297 g) and $Mn(NO_3)_2 \cdot 4H_2O$ (0.314 g) were dissolved in 50 mL of water under magnetic stirring until completely dissolved and then further mixed for another 15 min. Then $NH_4OH$ (80 mL) was added to the metal ions solution and mixed under continuous stirring for 30 min. Afterword, the solution was transferred to a closed Teflon lined container and placed in a stainless-steel autoclave and hydrothermal heated at 160 °C for 6 h. After cooling down to room temperature, the black colloidal $Co_{0.5}Mn_{0.5}Fe_2O_4$ magnetic nanoparticles were removed with a permanent magnet and were washed three times with DI water and ethanol. The magnetic powder was then freeze dry.

## 2.3 Preparation of silica-coated cobalt–manganese nanoferrite ($Co_{0.5}Mn_{0.5}Fe_2O_4$) (CoMnF@Si) (MagSi) particles

Silica-coated magnetic nanoparticle ($CoMnFe@SiO_2$) (MagSi) were synthesized via the Stöber process. In a typical experiment, 200 μL of magnetic nanoparticles (CoMnF) were added in a 7.2 mL mixture solution of ethanol and deionized water (the ratio of the two being 1 : 1 ethanol : water) under sonication. Then, 75 μL of TEOS (tetraethyl orthosilicate ($Si(OC_2H_5)_4$)) and 800 μL of $NH_4OH$ were added into the solution, respectively. The reacted mixture was further sonicated at room temperature for 1 h. After 1 h of reaction time, the brown silica-coated magnetic nanoparticles were obtained and washed 2 times using DI water under centrifugation at 12 000 rpm for 15 min. The supernatant was removed and the nanoparticles were collected and re-dispersed in 10 mL of DI water, freeze dried and kept in refrigerator (∼4 °C) for further used. The results are the $CoMnF@SiO_2$ (MagSi) nanoparticles.
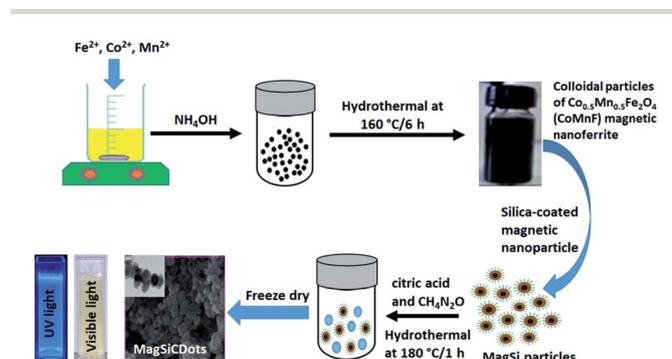


**Fig. 1** Illustration of the design and synthesis magneto-fluorescent of MagSiCDots nanoparticles.

## 2.4 Prepared magneto-fluorescence (CoMnF@Si@CDs) (MagSiCDots) nanoparticles

Magneto-fluorescence nanoparticles (CoMnF@Si@CDs) (MagSiCDots) are obtained by combining the carbon dots (CDots) with the silica-coated Co–Mn ferrite ($CoMnFe@SiO_2$) (MagSi) via a facile hydrothermal method. In a typical experiment, 2.5 mL of CoMnF@Si@CDs, 1 g citric acid and $CH_4N_2O$ (2 g) were dissolved in 7.5 mL of DI water under stirring and then stirred for another 30 min. Afterword, the solution was transferred to a sealed Teflon liner container and placed in a stainless-steel autoclave and heated at 180 °C for 1 h. After cooling down to room temperature, the dark green slurry of MagSiCDots was collected with a permanent magnet. The obtained MagSiCDots nanoparticles obtained by freeze dry.

## 2.5 Characterization of the materials

The morphologies and elemental analysis of the as-prepared samples were performed using a field emission scanning electron microscopy (FESEM-EDS) (Hitachi, SU5000) and a transmission electron microscopy (TEM) (JEOL, JEM-2100Plus, accelerating voltage 200 kV). The magnetic properties of $Co_{0.5}Mn_{0.5}Fe_2O_4$, MagSi and MagSiCDots particles were measured using VSM (vibrating sample magnetometer, Lakeshore, Model 4500). The magnetization ($M_S$) versus applied magnetic field ($H$) curve was measured at room temperature with magnetic field up to 10 000 Oe. Thermogravimetric analyses (TGA) were performed using Thermogravimetric Analyzer (Shimadzu, DTG-60AH) at a heating rate 20 °C $min^{-1}$ in a flowing nitrogen atmosphere from 25 to 800 °C. To determine the surface chemical composition on the as-prepared samples, X-ray photoelectron spectroscopy (XPS) (K-Alpha 1063, Thermo Fisher Scientific) was used. The hydrodynamic size and surface charge of the nanoparticles has been studied using Dynamic Light Scattering (DLS) technique. Fluorescence lifetime was measured with a F990 fluorescence spectrometer (Edinburgh Instruments Ltd. U.K.).

## 2.6 General procedure for fluorescent detection of $H_2S$

A stock solution of $H_2S$ was prepared using 0.01 M $Na_2S$ as the source and diluted properly to obtain a series of different concentration solutions (0.2, 0.5, 1, and 2 μM). In a cuvette, 1.9 mL of above stock solution of MagSiCDots (1.5 mg $mL^{-1}$) was treated with 100 μL $H_2S$ stock solution at various concentrations with gentle mixing for 1 min. The mixture was subjected to fluorescence measurement. To assess the time dependent fluorescent $H_2S$ assay (5, 10, 15, 20, 25, 30, 35, 40, 45, 50, 55, 60, 65, 70, 75, 80, 85 and 90 min), 1.5 mg $mL^{-1}$ of MagSiCDots were incubated with 0.5 μM $H_2S$. Every sample was prepared and measured as described previously.

## 2.7 Magnetic heating and the specific absorption rate (SAR) measurements

The magnetic heating efficiency of MagSiCDots particles was evaluated by using a homemade alternating magnetic field (AMF) current generator having a power output of 5 kW

generating AMF of 129 kHz. For the magnetic heating measurements, 3 mL of the dispersed solutions of MagSiCDots particles in water with the concentration of 1 mg mL$^{-1}$ was placed inside the middle of 6-turn copper coil of 30 mm in diameter and 65 mm in length and a current was passed through a coil. The heat generated by the sample was determined by measuring the change in temperature of solution (using the alcohol thermometer placed at the center of suspension) as function of time up to 60 min.

### 2.8  *In vitro* cytotoxicity of magneto-fluorescence (CoMnF@Si@CDs) (MagSiCDots) nanoparticles

To evaluate the biocompatibility, human cervical cancer cells (HeLa cells) was used. The cultured cells were kept at 37 °C in a humidified CO$_2$ incubator during cultivation and during the experiments. For the cyto-toxicity analysis, HeLa cells were seeded in 96-well plates and then incubated with MagSiCDots suspensions in media at a concentration of 0, 20, 40, 60, 80 and 100 μg mL$^{-1}$. The percentage of cell viability was assessed by MTT assay in which 100 μL 3-(4,5-dimethylthiazol-2-yl)-2,5-diphenyl-tetrazolium bromide (MTT) solution was added into the well and the samples were incubated for another 2 h then the absorbance was measured with a microplate reader (Varioskan LUX, Thermo Fisher Scientific Inc. Waltham, Massachusetts, USA) at the excitation and emission fluorescence from each well. The cytotoxicity was expressed as the percentage of cell viability compared with that of control group.

### 2.9  *In vivo* cytotoxicity test (zebrafish toxicity assay)

**Zebrafish husbandry.** Adult zebrafish (*Danio rerio*) were raised in a recirculation system (AAB-074, Yakos65, Taiwan) under a photoperiod of 14/10 h (day/night) under optimum water conditions, *i.e.*, temperature (28.5 ± 1 °C), pH (6.0–8.0), conductivity (300–700 μS) and DO (>6 mg L$^{-1}$). Embryos were obtained from mating of the fishes and were raised in egg water (0.03% (w/v) sea salt in DI water). Fertilized (normal) embryos obtained at 4 hours post-fertilization (hpf) were selected for studying using a stereomicroscope (SZX16, Olympus, Tokyo, Japan). The experimental procedures used were approved by the NSTDA Institutional Animal Care and Use Committee (No. 005-2562).

The zebrafish toxicity assay used follows the Organization for Economic Co-operation and Development guideline 236 (OECD 236, 2013). The MagSiCDots particles were prepared as a stock solution by adding the particles to DI water and sonicated for 10 min. For test, the stock solutions were diluted in egg water to final concentrations of 20, 40, 60, 80 and 100 μg mL$^{-1}$ and sonicated for 10 min. Twenty good quality embryos were exposed with 2 mL for each test solution in a 12-well culture plate and 2 mL of egg water was used as a negative control. Each test solution was vortexed for 20 s before adding to the wells. The experiment was performed as 3 replicates. The plates were incubated at 28.5 ± 1 °C under a photoperiod of 14/10 h day/night for up to 72 h. Every 24 h the test solutions were refreshed and dead embryos were removed. The number of dead was observed after expose for 24, 48, and 72 h.

### 2.10  Statistical analysis

Data were expresses as mean ± standard deviation (SD) of experiments performed in triplicate. The statistical significance between each test solution and control were determined by using one-way analysis of variance (ANOVA) followed by Tukey's test to compare the differences between groups and $p < 0.05$ was regarded as statistically significant.

## 3.  Results and discussion

### 3.1  Characterization of CoMnFe@Si@CDs

Morphology of the nanoparticles of magnetic nanoferrite, MagSi and magneto-fluorescent (MagSiCDots) were investigated by SEM and TEM. The SEM image of a MagSiCDots nano hybrid is shown in Fig. 2(a). It shows that the nanoparticle has a spherical morphology with an average size of 0.1–0.2 μm. The energy dispersive spectrum (EDS) analysis of MagSiCDots nanoparticle is illustrated in Fig. 2(b). The Kα of elements are observed in the spectrum which is confirmed that the presence of Co, Mn, Fe, Si, O and C elements in the sample. The lower metals intensity and higher for Si and C EDS intensities revealed that the presence of C and Si shell and attributed to the magnetic CoMnF nanoparticle in the core and coexisting silicon-CDots shell. To obtain more insights of the nano-structure of synthesis materials, TEM image of the magnetic nanoferrite (CoMnF) particles were taken (see Fig. 2(c)). The CoMnF particles prepared by hydrothermal have the average particle size about 5–10 nm. Fig. 2(d) shows the silica-coated magnetic nanoparticle (CoMnF@SiO$_2$) (MagSi). These images clearly show that they have a core–shell structure with particle diameter of 150 nm. The dark core of the CoMnF and the gray silica shells of thickness 30–40 nm were clearly observed. As seen in Fig. 2(e), the carbon dots (CDots) with particle diameter of 2–3 nm were uniform distribution in the nanoparticles. The TEM image of magneto-fluorescent nanoparticles (MagSiCDots) shown in Fig. 2(f) show that the small black CDots particles with particle diameter of 2–5 nm are densely dispersed on the shell of MagSi surface. This indicates a successful synthesis of the carbon dots (CDots) with silica-coated cobalt–manganese
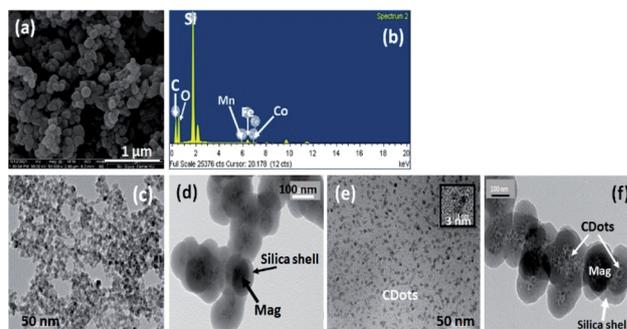


**Fig. 2** SEM (a) and EDS (b) images of MagSiCDots. TEM images of the synthesized (c) magnetic nanoferrite (CoMnF), (d) silica–coated magnetic nanoparticle (CoMnF@SiO$_2$) (MagSi), (e) carbon dots (CDots), and (f) magneto-fluorescent nanoparticles (CoMnF@Si@CDots) (MagSiCDots).

nanoferrite (Co$_{0.5}$Mn$_{0.5}$Fe$_2$O$_4$) (MagSiCDots) using the facile hydrothermal method.

A thermogravimetric analyzer (TGA) was used to confirm the coating formation and to estimate the binding efficacy of SiC-Dots on the surface of CoMnF nanoferrite. The TGA measurements were carried out by weighting a powder sample of 5 mg and loading them onto an alumina pan. The mass change under the temperature scan from 25 to 800 °C at a heating rate 15 °C min$^{-1}$ and under a nitrogen flow was monitored and recorded. Fig. 3 shows the result of TGA on nanoparticles at the range of 25–800 °C. CoMnF are stable up to 800 °C with a weight loss of *ca.* 12% in the range of 25 to 300 °C that could be attributed to the loss of adsorbed water, organic species, and residual regent used in synthesis process. After silica coating, MagSi shows weight loss of *ca.* 15% after heating up to 800 °C. 3% of weight loss increased as compared with those of CoMnF solely can confirm the success of silica coating. Also, TG thermogram of MagSi started to decompose from the beginning of the experiment to *ca.* 400 °C (*ca.* 12%). This degradation is attributed to the decomposition of hydroxyl groups and silane coupling agent attached for the fabrication of silica layer and physically adsorbed water and other organic species (from 25 to 200 °C). For MagSiCDots, TG thermogram shows 3 steps decompositions started from 25 to 800 °C with overall weight of *ca.* 20%. This can confirm the present of silica and carbon dots in the structure. The increased weight loss could be attributed to the degradation of carbon dots which is completely decomposed above 700 °C under atmospheric condition. No weight loss could be observed above 800 °C for MagSiCDots and the remnant is cobalt–manganese nanoferrites (Co$_{0.5}$Mn$_{0.5}$Fe$_2$O$_4$) and silica (SiO$_2$) which is stable above 800 °C.[38]

The surface charge of synthesized particles was determined using zeta potential measurements. As seen in Fig. 4, the zeta potentials of magnetic nanoferrite, MagSi, CDots and MagSiC-Dots were −19.1, −32.1, −16.1, and −35.5 mV, respectively. The negative charged surface of magnetic nanoferrite (CoMnF) could be due to the formation of Mn–Co–Fe oxide layer. After the carbon dots were combined with the silica-coated cobalt–
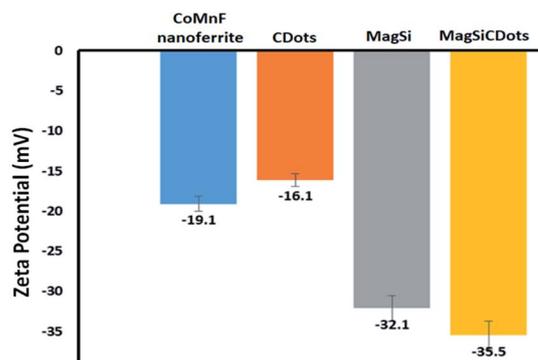


Fig. 4 The zeta potentials of magnetic nanoferrite (CoMnF), silica-coated magnetic nanoparticle (CoMnFe@SiO$_2$) (MagSi), carbon dots (CDots), and magneto-fluorescent nanoparticles (CoMnF@Si@CDots) (MagSiCDots).

manganese nano ferrite (MagSiCDots), the high negative value of the nanoparticles decreased to −32.1 mV for MagSi and to −35.5 mV for MagSiCDots demonstrating a successfully modified silinol (Si–O) functional group formation on the CoMnF surface and resulted in the anchoring of the CDots on the MagSi surface, respectively. The high negative surface charge value led to MagSiCDots particles being well dispersed in aqueous solution due to accompanying electrostatic repulsion the particles.

The chemical element composition of MagSiCDots was analyzed by XPS, with the results shown in Fig. 5. XPS survey analysis (Fig. 5(a)) shows that the as-prepared powders consist of C 1s, O 1s, Si 2p and N 1s elements and low signals of Fe 2p, Co 2p and Mn 2p elements. The lower intensities of Fe, Co and Mn are observed in the carbon dots (CDots) and silica-coated cobalt–manganese nanoferrites confirm that the CoMnF nanoparticles are completely coated by the SiCDots. Fig. 5(b) shows the high-resolution spectrum of C with the corresponding fitted curves. There are three functional groups attributed to the C–C, C–O and O=C–N at the binding energy of 285, 286 and 287.4 eV, respectively, which indicates that the MagSi shell
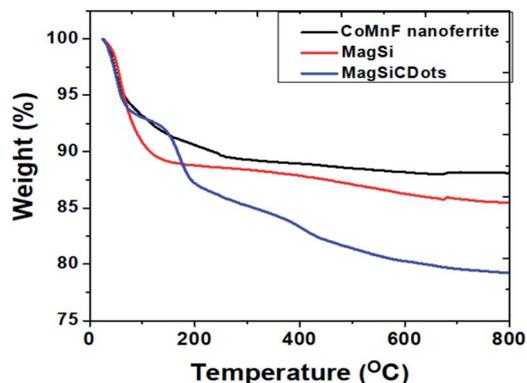


Fig. 3 TGA curves of the magnetic nanoferrite (CoMnF), silica-coated magnetic nanoparticle (CoMnF@SiO$_2$) (MagSi), carbon dots (CDots), and magneto-fluorescent nanoparticles (CoMnF@Si@CDots) (MagSiCDots).
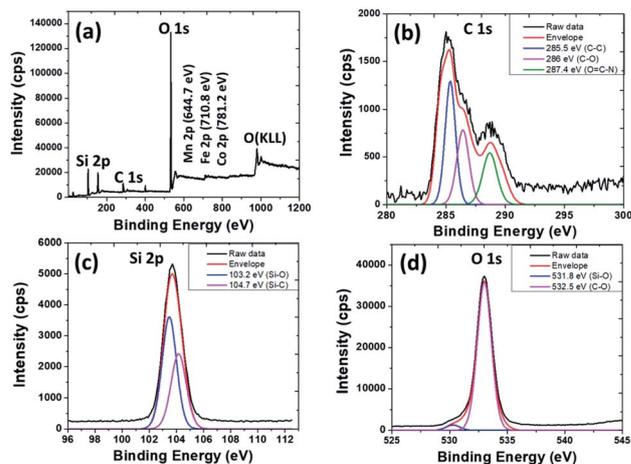


Fig. 5 XPS spectra of the as-prepared MagSiCDots nanoparticles; (a) survey spectra, (b) C 1s, (c) Si 2p and (d) O 1s.

contained CDots. The two main peaks of Si 2p (Fig. 5(c)) confirms the existence of the Si–O and Si–C bonding with the binding energy of 103.2 eV and 104.7 eV, respectively.[24,25] The O 1s spectrum seen in Fig. 5(d) shows two notable peaks at a binding energy of 532.5 eV and 531.8 eV corresponding to the Si–O bond in silica and oxygen atom in the C–O bond, respectively.[25,39] These finding indicates that the particles contain $SiO_2$ and the coexisting silicon-CDots which are on the surface of MagSiCDots particles. By XPS analysis reveal that amounts of hydrophilic functional groups exist on the surface of MagSiC-Dots nanoparticles, such functional groups are convenience for further combination of different biomolecules (drug or proteins) in drug delivery system.[24]

Magnetic behaviors of the particles were measured by VSM with the behaviors shown in Fig. 6. As seen from VSM result, a narrow hysteresis loop is observed (the coercive field ($H_c$) of the as-prepared nanoparticles was close to 0 Oe), indicating that the synthesized magnetic particles exhibited super-paramagnetic behaviour at room temperature. The saturation magnetization ($M_S$) values of CoMnF nanoferrite was 58.33 emu $g^{-1}$ and found to be comparable to previous work.[25] This result implies that this standard hydrothermal method standard hydrothermal method is capable of producing highly crystalline and phase-pure nanoparticles. The magnetization of MagSi and MagSiCDots were 22.03 and 11.6 emu $g^{-1}$, respectively. The reduction of the magnetization after the silica and CDots coating is due to the diamagnetic in nature of SiCDots layer being grafted on the CoMnF nanoferrite surface. This grafting provides for more magnetic shielding of the CoMnF nano-ferrite.[25] In spite of $M_S$ values being lowered by the silica and CDots coating, the particles still maintained their strong magnetism under applied magnet.

The optical properties of the synthesized magneto-fluorescent nanoparticles (MagSiCDots) were also investigated. The dispersed of MagSiCDots in solution exhibited a green-yellow colour glow under daylight illumination and emit blue light under UV stimulation (Fig. 7(a)). The
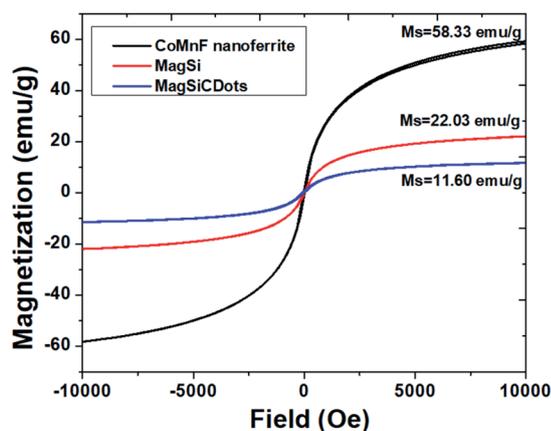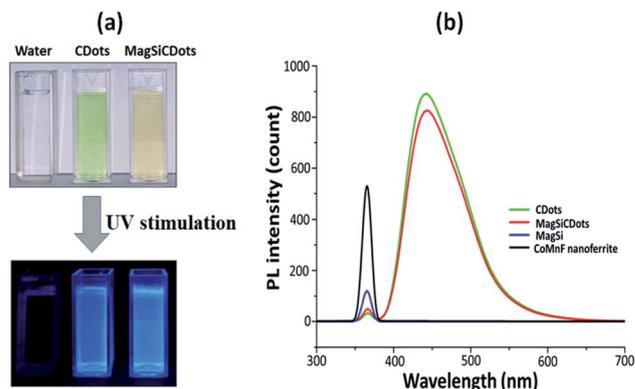


Fig. 7 (a) Digital images of water, CDots, and MagSiCDots in water under the day light and UV light. (b) Fluorescence spectra of CDots, MagSiCDots, MagSi, and CoMnF nanoferrite at excitation wavelength of 365 nm.

fluorescence spectra of CDs, CoMnF nanoferrite, MagSi and MagSiCDots nanoparticles are showed in Fig. 7(b). As seen in the fluorescence spectra of CDs and MagSiCDots nanoparticles, both showed emission at a wavelength of about 442.5 nm under an excitation wavelength of 365 nm. Meanwhile, the fluorescence spectra of CoMnF nanoferrite and MagSi were not observed at the same excitation wavelength. The present fluorescence of MagSiCDots was good relation with that of CDots indicating that a successfully modified carbon dots combination with MagSi particles.

## 3.2 The fluorescence response of H2S sensing with MagSiCDots

To investigate the sensitivity of MagSiCDots nanoparticles for detecting $H_2S$, the fluorescence emission after incubation of different concentration of $H_2S$ (0.2–2 μM) for 60 s was measured. As seen in Fig. 8(a), the fluorescence intensity of



Fig. 6 Room temperature magnetic hysteresis loops of magnetic nanoferrite (CoMnF), silica-coated magnetic nanoparticle (CoMnF@SiO2) (MagSi), carbon dots (CDots), and magneto-fluorescent nanoparticles (CoMnF@Si@CDots) (MagSiCDots).
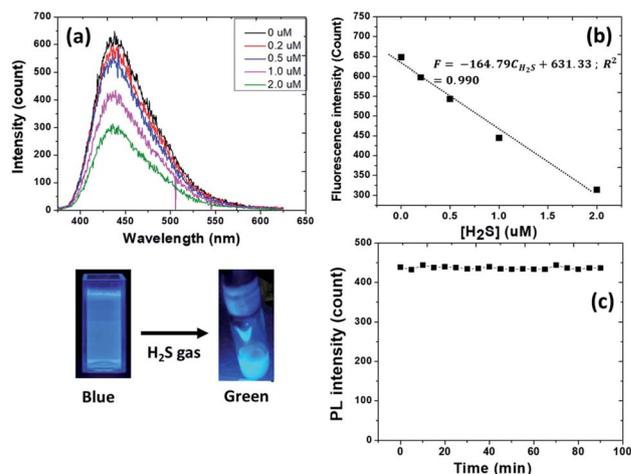


Fig. 8 (a) Fluorescence spectra of MagSiCDots upon the addition of different $H_2S$ concentrations. (b) Linear relationship between fluorescence intensity of MagSiCDots and $H_2S$ concentration. (c) The time dependent profile of fluorescent signal observed from $H_2S$ assay.

aqueous solution at 442.5 nm gradually decreased as the concentration of H$_2$S in the solution increased. The colour of solution changed from blue to blue-green light emission (inset figure). As illustrated in Fig. 8(b), the fluorescence intensity had a good linearly to the concentration. The linear relationship with the H$_2$S concentration in range of 0.2–2 μM is

$$F = -164.79C_{H_2S} + 631.33; R^2 = 0.990,$$

where $F$ is the fluorescence intensity, $C$ is the concentration of H$_2$S and $R$ is the correlation coefficient. The limit of detection (LOD) of H$_2$S by our MagSiCDots particles is $3\sigma/K$ (where $\sigma$ is the standard deviation measurements of blank solution on the fluorescence intensity at 442.5 nm and $K$ indicated the slope of the linear curve) was 0.26 μM and remain stable after at least 90 min (Fig. 8(c)). This detection limit demonstrates that the MagSiCDots nanoparticles are within the detection requirements of H$_2$S in such things as living cells or biological samples.[40]

### 3.3 Evaluation on heating ability

To evaluate the synthesized particles as a promising potential candidate for hyperthermia treatment of cancer, the rise in temperature as a function of time was measured. Fig. 9 shows the temperature *versus* time of the as-prepared Co$_{0.5}$Mn$_{0.5}$Fe$_2$O$_4$ (CoMnF) nanoferrite and MagSiCDots particles subject to an AMF. From the observation, the curve (graph in Fig. 9) shows a rising temperature of solution of the nanoferrite particles having a concentration of 1 mg mL$^{-1}$ when they are exposed to the AMF for 30 min. Obviously, the CoMnF nanoferrite shows a final temperature of 47.5 °C (which is above the range 42–44 °C suitable for the hyperthermia treatment) in 30 min while the temperature obtained when the MagSiCDots particles is about 36 °C. The actual temperature rise is found to be lower when MagSiCDots particles are present than the temperature will be when the CoMnF nanoferrite of the same concentration

are present. The reason for that the concentration of the magnetic particles in the CoMnF only is higher than that when solution contains the MagSiCDots nanoparticles. This would lead to the increased particle–particle interactions in the former and thus increase the exchange coupling energy and affect the induction heating.[41–43]

The hyperthermia performance is measured by the specific absorption rate (SAR) which is calculated from the heating efficiency of the nanoparticles from the formula given below:

$$\text{SAR (W g}^{-1}) = [C_w/m] \times [dT/dt] \tag{1}$$

where $C_w$ is the specific heat capacity (4.186 J g$^{-1}$ °C$^{-1}$) and $m$ is the magnetic particle concentration. $dT/dt$ is the rate of temperature rise and was obtained by fitting the heating curve to the phenomenological Box–Lucas model (eqn (2)), which is applicable for calorimetric measurements under nonadiabatic conditions.

$$T = T_0 + T_{max}(1 - e^{-Bt}) \tag{2}$$

where $T_0$ is the nonzero starting temperature, $T_{max}$ is the maximum temperature difference in the heating curve, and $B$ is the fitting parameter of the curve. The product ($T_{max} \times B$) is the rate. Based on this situation, the SAR calculated from eqn (1) and (2) for CoMnF nanoferrite and MagSiCDots are 69.81 and 28.26 W g$^{-1}$, respectively. Based on these results, it can be seen that the CoMnF nanoferrite exhibits higher heating capacity compared to that of the MagSiCDots. The change in the SAR value of CoMnF after coating might be attributed to the SiCDots shell which is expected to be an insulating layer which reduces the energy transfer from the CoMnF nanoferrite to the media. Despite the presence of the SiCDots shell, the SAR of MagSiC-Dots in suspension reached 28.26 W g$^{-1}$. This demonstrates that the as-prepared CoMnF coated by SiCDots are potential candidate for being the heat source in magnetic hyperthermia treatment of cancer.

### 3.4 *In vitro* cytotoxicity characterization

The cytotoxicity of the MagSiCDots in HeLa cells was evaluated by using the MTT assay carried out after incubation for 24 h. As
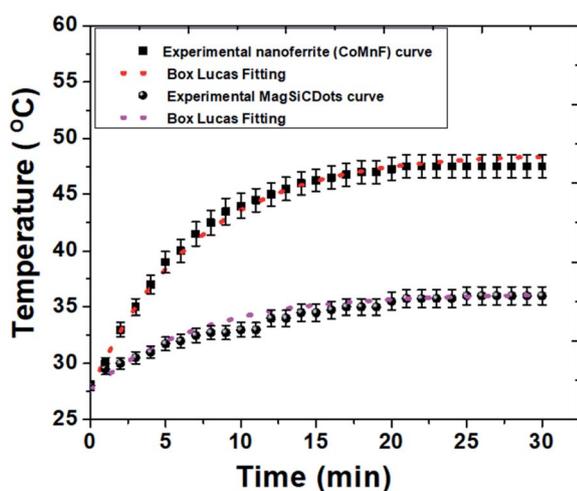


**Fig. 9** Induction heating curve of CoMnF nanoferrite and MagSiCDots particles with Box−Lucas fitting operating at 5 kW with 129 kHz. The results are presented as mean ± SE (*n* = 3).
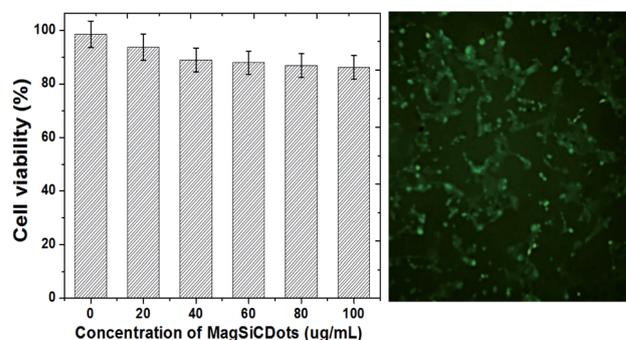


**Fig. 10** Cell viability by MTT and fluorescence-based assay. HeLa cell is incubated with different concentrations (0, 20, 40, 60, 80 and 100 μg mL$^{-1}$) of MagSiCDots. The results are presented as mean ± SE (*n* = 3).
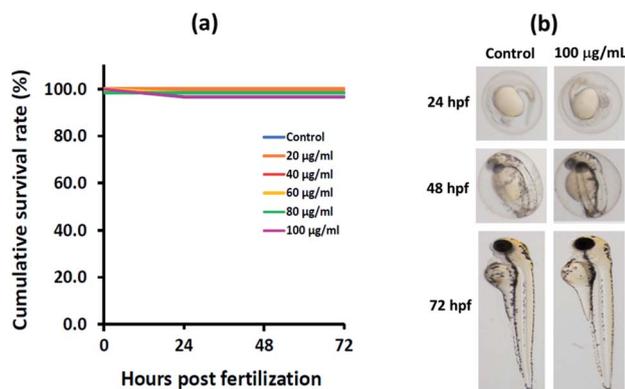
**Fig. 11** Survival rates of zebrafish embryos exposed to different concentrations ($\mu$g mL$^{-1}$) of MagSiCDots at 24, 28 and 72 hours post-fertilization (hpf) (a). (b) Digital photographs of zebrafish embryos at different stages of growth in solutions containing exposed to different concentrations ($\mu$g mL$^{-1}$).

shown in Fig. 10, no more than 80% of HeLa cells was viable for concentration of the MagSiCDots between 0–20 $\mu$g mL$^{-1}$. The cell viability determined from a MTT assay slowly decreased from $98.56 \pm 4.93$ to $97.74 \pm 4.80$ to $87.88 \pm 4.39$ to $86.85 \pm 4.34$ and to $85.12 \pm 4.25\%$ as the concentrations increased from 0 (control) to 20 to 40 to 60 to 80 and to 100 $\mu$g mL$^{-1}$, respectively. From these results, it is seen that the synthesized MagSiCDots particles have low cytotoxicity to living cells for concentrations below 100 $\mu$g mL$^{-1}$. Based on the fluorescence-based assay, treatment with MagSiCDots nanoparticles at a concentration of 100 $\mu$g mL$^{-1}$ shows much less early apoptotic cells which are interacting with cell membranes (which are seen as being green and had the strongest fluorescence intensity).

### 3.5 *In vivo* cytotoxicity characterization in zebrafish

The effects of synthesized particles on zebrafish embryo survival was done to assess the safety of MagSiCDots particles on zebrafish embryo exposed to nanoparticle at 0, 20, 40, 60, 80, and 100 $\mu$g mL$^{-1}$ up to 72 hpf. The survival rates of zebrafish embryos after being treated with particles did not show significant difference compared to the control group (Fig. 11(a)). To evaluate the effects of the particles on zebrafish morphology, zebrafish embryos/larvae were observed and documented. Representative images of the embryos/larvae at 24, 48, and 72 hpf from the exposure to MagSiCDots particles are presented in Fig. 11(b). During time points, no malformation of zebrafish embryos/larvae was observed in the MagSiCDots treated groups. The conclusion for the cytotoxic effect of as-prepared MagSiCDots particles on *in vivo* in zebrafish assay, as seen in this work, is that after the exposure, to MagSiCDots particles did not induce mortality or malformation of zebrafish embryos/larvae.

## 4.    Conclusions

In summary, we have successful synthesized biocompatible CDots-loaded silica coated nanoferrite (MagSiCDots) *via* facile hydrothermal method. This particle was characterized in terms of physico-chemical, magnetic property, fluorescence, H$_2$S detection, hyperthermia including cytotoxicity. The MagSiC-Dots have a core–shell structure with the CDots being well dispersed on the surface of the MagSi particles. The saturation magnetization of the particles was 11.6 emu g$^{-1}$. The synthesized particles exhibited good stability while in an aqueous solution and they emitted a blue light emission at the wavelength of 442.5 nm. Their use as a potential fluorescent sensor for hydrogen sulfide (H$_2$S) detection and the heat source for the hyperthermal treatment of diseases was assayed by establishing that the intensities of the fluorescence emission by the MagSiCDots nanoparticles are linearly dependent on the concentration of the H$_2$S in the range of concentration 0.2–2 $\mu$M with the LOD is 0.26 $\mu$M which is in the range of H$_2$S generated by some diseases. Meanwhile, the possibility to hyperthermia application, is possible since the as-prepared MagSiCDots nanoparticles in AMF have a specific absorption rate (SAR) of 28.25 W g$^{-1}$. The *in vitro* cytotoxicity of MagSiCDots was tested on HeLa cells line and observed by MTT assay. Experimental result showed that MagSiCDots had low cytotoxicity with the different concentrations. In addition, MagSiCDots nanoparticles exhibited no toxicity to the zebrafish embryos up to 100 $\mu$g mL$^{-1}$ exposure concentration, suggesting remarkable *in vivo* biocompatibility. From these reports, the magneto-fluorescence nanoparticles consisting of carbon dots (CDots) combined with silica-coated cobalt–manganese nanoferrite (Co$_{0.5}$Mn$_{0.5}$Fe$_2$O$_4$) (CoMnF@Si@CDs) (MagSiCDots) could serve as a platform particle for sensitive fluorescent sensor and potential candidate for various biomedical applications such as a potential heat source for magnetic hyperthermia applications.

## Conflicts of interest

There are no conflicts to declare.

## Acknowledgements

## References

1  A. Tufani, A. Qureshi and J. H. Niazi, Iron oxide nanoparticles based magnetic luminescent quantum dots (MQDs) synthesis and biomedical/biological applications: a review, *Mater. Sci. Eng., C*, 2021, **118**, 111545.

2  C. Y. Wen, H. Y. Xie, Z. L. Zhang, L. L. Wu, J. Hu, M. Tang, M. Wu and D. W. Pang, Fluorescent/magnetic micro/nanospheres based on quantum dots and/or magnetic nanoparticles: preparation, properties, and their applications in cancer studies, *Nanoscale*, 2016, **8**, 12406–12429.

3 G. A. Marcelo, C. Lodeiro, J. L. Capelo, J. Lorenzo and E. Oliveira, Magnetic, fluorescent and hybrid nanoparticles: From synthesis to application in biosystems, *Mater. Sci. Eng., C*, 2020, **106**, 110104.

4 B. Fernández, N. Gálvez, R. Cuesta, A. B. Hungría, J. J. Calvino and J. M. Domínguez-Vera, Quantum Dots Decorated with Magnetic Bionanoparticles, *Adv. Funct. Mater.*, 2008, **18**, 3931–3935.

5 R. Gui, Y. Wang and J. Sun, Encapsulating magnetic and fluorescent mesoporous silica into thermosensitive chitosan microspheres for cell imaging and controlled drug release *in vitro*, *Colloids Surf., B*, 2014, **113**, 1–9.

6 Q. Ma, Y. Nakane, Y. Mori, M. Hasegawa, Y. Yoshioka, T. M. Watanabe, K. Gonda, N. Ohuchi and T. Jin, Multilayered, core/shell nanoprobes based on magnetic ferric oxide particles and quantum dots for multimodality imaging of breast cancer tumors, *Biomaterials*, 2012, **33**, 8486–8494.

7 A. Qureshi, A. Tufani, G. Corapcioglu and J. H. Niazi, CdSe/CdS/ZnS nanocrystals decorated with $Fe_3O_4$ nanoparticles for point of-care optomagnetic detection of cancer biomarker in serum, *Sens. Actuators, B*, 2020, **321**, 128431.

8 J. Gao, H. Gu and B. Xu, Multifunctional magnetic nanoparticles: Design, synthesis, and biomedical applications, *Acc. Chem. Res.*, 2009, **42**, 1097–1107.

9 D. Yoo, J.-H. Lee, T.-H. Shin and J. Cheon, Theranostic Magnetic Nanoparticles, *Acc. Chem. Res.*, 2011, **44**(10), 863–874.

10 Y.-W. Jun, J.-W. Seo and J. Cheon, Nanoscaling Laws of Magnetic Nanoparticles and Their Applicabilities in Biomedical Sciences, *Acc. Chem. Res.*, 2008, **41**(2), 179–189.

11 A. M. Wagner, J. M. Knipe, G. Orive and N. A. Peppas, Quantum dots in biomedical applications, *Acta Biomater.*, 2019, **94**, 44–63.

12 S. Filali, F. Pirot and P. Miossec, Biological Applications and Toxicity Minimization of Semiconductor Quantum Dots, *Trends Biotechnol.*, 2020, **38**(2), 163–177.

13 C. T. Matea, T. Mocan, F. Tabaran, T. Pop, O. Mosteanu, C. Puia, C. Iancu and L. Mocan, Quantum dots in imaging, drug delivery and sensor applications, *Int. J. Nanomed.*, 2017, **12**, 5421–5431.

14 W. M. Girma, M. Z. Fahmi, A. Permadi, M. A. Abatea and J.-Y. Chang, Synthetic strategies and biomedical applications of I–III–VI ternary quantum dots, *J. Mater. Chem. B*, 2017, **5**, 6193–6216.

15 M. Farshbaf, S. Davaran, F. Rahimi, N. Annabi, R. Salehi and A. Akbarzadeh, Carbon quantum dots: recent progresses on synthesis, surface modification and applications, *Artif. Cells, Nanomed., Biotechnol.*, 2018, **46**(7), 1331–1348.

16 Y. Wang and A. Hu, Carbon quantum dots: synthesis, properties and applications, *J. Mater. Chem. C*, 2014, **2**, 6921–6939.

17 W. Su, H. Wu, H. Xu, Y. Zhang, Y. Li, X. Li and L. Fan, Carbon dots: a booming material for biomedical applications, *Mater. Chem. Front.*, 2020, **4**, 821–836.

18 H. Wang, J. Shen, Y. Li, Z. Wei, G. Cao, Z. Gai, K. Hong, P. Banerjeea and S. Zhou, Magnetic iron oxide-fluorescent carbon dots integrated nanoparticles for dual-modal imaging, near-infrared light-responsive drug carrier and photothermal therapy, *Biomater. Sci.*, 2014, **2**, 915–923.

19 I. Perelshtein, N. Perkas, S. Rahimipour and A. Gedanken, Bifunctional Carbon Dots-Magnetic and Fluorescent Hybrid Nanoparticles for Diagnostic Applications, *Nanomaterials*, 2020, **10**, 1384.

20 A. Pramanik, S. Jones, F. Pedraza, A. Vangara, C. Sweet, M. S. Williams, V. Ruppa-Kasani, S. E. Risher, D. Sardar and P. C. Ray, Fluorescent, Magnetic Multifunctional Carbon Dots for Selective Separation, Identification, and Eradication of Drug-Resistant Superbugs, *ACS Omega*, 2017, **2**, 554–562.

21 H. Yao, L. Su, M. Zeng, L. Cao, W. Zhao, C. Chen, B. Du and J. Zhou, Construction of magnetic-carbon-quantum-dots-probe-labeled apoferritin nanocages for bioimaging and targeted therapy, *Int. J. Nanomed.*, 2016, **11**, 4423–4438.

22 M. L. Bhaisare, G. Gedda, M. S. Khan and H.-F. Wu, Fluorimetric detection of pathogenic bacteria using magnetic carbon Dots, *Anal. Chim. Acta*, 2016, **920**, 63–71.

23 S. Mohapatra, S. Sahu, S. Nayak and S. K. Ghosh, Design of $Fe_3O_4$@$SiO_2$@Carbon Quantum Dot Based Nanostructure for Fluorescence Sensing, Magnetic Separation, and Live Cell Imaging of Fluoride Ion, *Langmuir*, 2015, **31**, 8111–8120.

24 X. Li, W. Wang, Q. Li, H. Lin, Y. Xu and L. Zhuang, Design of $Fe_3O_4$@$SiO_2$@$mSiO_2$-organosilane carbon dots nanoparticles: Synthesis and fluorescence red-shift properties with concentration dependence, *Mater. Des.*, 2018, **151**, 89–101.

25 Y. Guan, Y. Yang, X. Wang, H. Yuan, Y. Yang, N. Li and C. Ni, Multifunctional $Fe_3O_4$@$SiO_2$-CDs magnetic fluorescent nanoparticles as effective carrier of gambogic acid for inhibiting VX2 tumor cells, *J. Mol. Liq.*, 2021, **327**, 114783.

26 A. Tiwari, N. C. Verma, S. Turkkan, A. Debnath, A. Singh, G. Draeger, C. K. Nandi and J. K. Randhawa, Graphitic Carbon Coated Magnetite Nanoparticles for Dual Mode Imaging and Hyperthermia, *ACS Appl. Nano Mater.*, 2020, **3**, 896–904.

27 M. R. Filipovic, J. Zivanovic, B. Alvarez and R. Banerjee, Chemical Biology of $H_2S$ Signaling through Persulfidation, *Chem. Rev.*, 2018, **118**, 1253–1337.

28 Y. Qian, L. Zhang, S. Ding, X. Deng, C. He, X. E. Zheng, H.-L. Zhu and J. Zhao, A fluorescent probe for rapid detection of hydrogen sulfide in blood plasma and brain tissues in mice, *Chem. Sci.*, 2012, **3**, 2920–2923.

29 H. Peng, Y. Cheng, C. Dai, A. L. King, B. L. Predmore, D. J. Lefer and B. Wang, A Fluorescent Probe for Fast and Quantitative Detection of Hydrogen Sulfide in Blood, *Angew. Chem., Int. Ed.*, 2011, **50**, 9672–9675.

30 K. Kashfi, The role of hydrogen sulfide in health and disease, *Biochem. Pharmacol.*, 2018, **149**, 1–4.

31 D. Giuliani, A. Ottani, D. Zaffe, M. Galantucci, F. Strinati, R. Lodi and S. Guarini, Hydrogen sulfide slows down progression of experimental Alzheimer's disease by targeting multiple pathophysiological mechanisms, *Neurobiol. Learn. Mem.*, 2013, **104**, 82–91.

32 C. Szabo, C. Coletta, C. Chao, K. Módis, B. Szczesny, A. Papapetropoulos and M. R. Hellmich, Tumor-derived hydrogen sulfide, produced by cystathionine-β-synthase, stimulates bioenergetics, cell proliferation, and angiogenesis in colon cancer, *Proc. Natl. Acad. Sci. U. S. A.*, 2013, **110**(30), 12474–12479.

33 T. Xu, N. Scafa, L.-P. Xu, S. Zhou, K. A. Al-Ghanem, S. Mahboob, B. Fugetsue and X. Zhang, Electrochemical hydrogen sulfide biosensors, *Analyst*, 2016, **141**, 1185–1195.

34 X. Zhang, W. Zhou, Z. Yuan and C. Lu, Colorimetric detection of biological hydrogen sulfide using fluorosurfactant functionalized gold nanorods, *Analyst*, 2015, **140**, 7443–7450.

35 T. Ubuka, T. Abe, R. Kajikawa and K. Morino, Determination of hydrogen sulfide and acid-labile sulfur in animal tissues by gas chromatography and ion chromatography, *J. Chromatogr. B: Biomed. Sci. Appl.*, 2001, **757**, 31–37.

36 N. Sanpo, J. Tharajak, Y. Li, C. C. Berndt, C. Wen and J. Wang, Biocompatibility of transition metal-substituted cobalt ferrite nanoparticles, *J. Nanopart. Res.*, 2014, **16**, 2510.

37 N. Sanpo, C. C. Berndt, C. Wen and J. Wang, Transition metal-substituted cobalt ferrite nanoparticles for biomedical applications, *Acta Biomater.*, 2013, **9**, 5830–5837.

38 J. Hong, J. Lee, C. Hong and S. Shim, Improvement of thermal conductivity of poly(dimethyl siloxane) using silica-coated multi-walled carbon nanotube, *J. Therm. Anal. Calorim.*, 2010, **101**, 297–302.

39 S. Zhao, S. Sun, K. Jiang, Y. Wang, Y. Liu, S. Wu, Z. Li, Q. Shu and H. Lin, *In Situ* Synthesis of Fluorescent Mesoporous Silica–Carbon Dot Nanohybrids Featuring Folate Receptor-Overexpressing Cancer Cell Targeting and Drug Delivery, *Nano-Micro Lett.*, 2019, **11**, 32.

40 J. Furne, A. Saeed and M. D. Levitt, Whole tissue hydrogen sulfide concentrations are orders of magnitude lower than presently accepted values, *Am. J. Physiol.*, 2008, **295**, R1479–R1485.

41 J. Mohapatra, M. Xing and J. P. Liu, Inductive Thermal Effect of Ferrite Magnetic Nanoparticles, *Materials*, 2019, **12**, 3208.

42 Z. Shaterabadi, G. Nabiyouni and M. Soleymani, Physics responsible for heating efficiency and self-controlled temperature rise of magnetic nanoparticles in magnetic hyperthermia therapy, *Prog. Biophys. Mol. Biol.*, 2018, **133**, 9–19.

43 I. M. Obaidat, V. Narayanaswamy, S. Alaabed, S. Sambasivam and C. V. V. Muralee Gopi, Principles of Magnetic Hyperthermia: A Focus on Using Multifunctional Hybrid Magnetic Nanoparticles, *Magnetochemistry*, 2019, **5**, 67.